

PAPER • OPEN ACCESS

Analyses of Deformation and Stress of Oil-free Scroll Compressor Scroll

To cite this article: Bin Peng *et al* 2017 *IOP Conf. Ser.: Mater. Sci. Eng.* **274** 012005

View the [article online](#) for updates and enhancements.

You may also like

- [Novel two-directional grid multi-scroll chaotic attractors based on the Jerk system](#)
Peng-Fei Ding, , Xiao-Yi Feng et al.
- [Scroll-growing/controlling chaotic attractors in cyclic Hopfield neural networks via memristive bridging](#)
Jian Chen, Zhuguan Chen, Quan Xu et al.
- [A general method for generating multi-scroll and multi-wing chaotic systems and its implementation of attractor reproduction](#)
Ping He, Hongwei Liu, Guodong Li et al.



ECS
The
Electrochemical
Society
Advancing solid state &
electrochemical science & technology

DISCOVER
how sustainability
intersects with
electrochemistry & solid
state science research

Analyses of Deformation and Stress of Oil-free Scroll Compressor Scroll

Bin Peng^{1,2,*}, **Yaohong Li**^{1,2,a}, **Shenxian Zhao**^{1,2,b}

¹ School of Mechanical and Electrical Engineering, Lanzhou University of Technology. Lanzhou, Gansu, China

² Wenzhou Pump& Valve Engineering Research Institute, Lanzhou University of Technology. Wenzhou, Zhejiang, China

*Corresponding author e-mail: pengb2000@163.com, ^a346574950@qq.com, ^b272629964@qq.com.

Abstract. The solid model of orbiting and fixed scroll is created by the Solidworks The deformation and stress of scrolls under gas force, temperature field, inertia force and the coupling field are analyzed using the Ansys software. The deformation for different thickness and height scroll tooth is investigated. The laws of deformation and stress for scrolls are gotten. The research results indicate that the stress and deformation of orbiting scroll are mainly affected by the temperature field. The maximum deformation occurs in the tooth head of scroll wrap because of the largest gas forces and the highest temperature in the tooth head of scroll wrap. The maximum stress is located in the end of the tooth, and the maximum stress of the coupling field is not the sum of loads. The scroll tooth is higher, and the deformation is bigger. The scroll tooth is thicker, and the deformation is smaller.

Key words: oil-free scroll compressor; scrolls; coupling; Ansys; deformation; stress

1. Introduction

Scroll compressor as a new type compressor, because of its simple structure, small volume, light weight, small vibration, low noise, less wearing parts, stable operation and many other advantages are widely used in air conditioning and pneumatic system. The pressure of the gas in the working chambers gradually increases with the rotation of the shaft, and the high pressure gas is discharged by the exhaust hole. The gas force working on the scrolls will cause the deformation of the scroll tooth of the compressor. The temperature of the gas in the working chambers increases and causes the thermal deformation of the scroll tooth; The rotation of the crankshaft drives the orbiting scroll of the compressor to rotate, and generated the inertial load field, resulting in the deformation of the scroll tooth; The assembly gap of the scrolls will change due to the deformation of the scroll tooth; The gap of the scroll will affect the efficiency of the scroll compressor, the gap is too large, leading to increased leakage will be increased with the large gap, and the friction will be increasing with small gap; Oil-free scroll compressor does not have lubricating oil for cooling and lubrication, the pressure and temperature of the gas in the working chambers are higher Compared with the oil lubricated compressor, and the deformation of the scroll is also greater; In order to ensure the normal operation



of the compressor and the assembly gap, it is very important to analyze the deformation of scroll compressor under the multi field load[1-4].

Many scholars in China have done a lot of analysis and Research on the deformation of scroll plates and scroll teeth of compressors. (Dan Jin, 2003.Huang L., 2006.Li Chao, 2013, 2015.Yin Jun, 2011.Guo R N., 2011.Wang J., 2012.Yang G Y., 2008). The existing researches are all about the analysis of the deformation of the scroll disk under the single load. However, in different practical conditions, the deformation of the scroll is different greatly.In this paper, therefore, considering the pressure field and temperature field of load, inertial load field and scroll tooth height, thickness of different influence factors, the analysis software Ansys is applied to analyze the deformation distribution of oil free scroll compressor, the analysis provides a theoretical basis for the design and assembly of machine performance, oil free scroll the scroll compressor.

2. Load analysis of Orbiting Scroll

2.1. Temperature load

When the scroll compressor works stably, the temperature of the scroll tooth rises uniformly from the suction chamber to the central exhaust chamber, while the gas is compressed. The temperature of the gas in the exhaust chamber of the compressor is calculated by equation (1) in the adiabatic process:

$$T_d = T_s \left(\frac{P_d}{P_s} \right)^{\frac{k-1}{k}} \quad (1)$$

In the analysis process, the variation of the temperature of the scroll tooth can be simplified as a linear distribution along the radius of the line of the generating teeth. The temperature of the scroll tooth gradually decreases along the radius of the profile line [13].

2.2. Gas force load

With the rotation of the spindle angle, the gas in the cavity is compressed more and more, and the pressure reaches the maximum value at the exhaust time. Therefore, the static structure analysis of the scroll tooth is selected. At this point, the volume and pressure of the gas in each cavity of the compressor are calculated by the following two formulas:

$$V = 2h \left(\frac{P}{2} - t \right) \int_{\phi_e - \theta^* - \theta}^{\phi_e - \theta} r_b d\phi \quad (2)$$

$$(0 \leq \theta \leq \phi_e - 2\pi - \theta^* - \varphi)$$

The instantaneous volume of each chamber of the compressor can be obtained by (1). If the compression of the gas is adiabatic, the gas pressure in the chamber i is:

$$p_i(\theta) = \left(\frac{V_s}{V_i(\theta)} \right)^k p_s \quad (3)$$

2.3. Inertial load

The scroll scroll compressor rotates in a rotational manner with respect to the stationary vortex disk, with r as the radius of gyration, resulting in inertial forces. The magnitude of the inertial force is calculated by the lower form:

$$Q = ma$$

$$a = r\omega^2 = r(2\pi n / 60)^2 \tag{4}$$

3. Finite element analysis of scroll plate

The 8 node hexahedron as the basic unit to analyze the geometric analysis of the orbiting scroll, which each node has x, y and z displacement in three directions and the occurrence of rotational degrees of freedom, the displacement of each node by the relation of shape functions to represent the [14]:

$$[U] = [N][d] \tag{5}$$

[d]——Analyze the displacement vectors of elements; [U]——Displacement vector of an object; [N]——Shape function vector.

From stress-strain relation:

$$[\sigma] = [D][\varepsilon] \tag{6}$$

[σ], [ε] is stress and strain matrix. [D]——Physical constant matrix.

$$[\sigma] = [\sigma_x, \sigma_y, \sigma_z, \tau_{yz}, \tau_{xz}, \tau_{xy}]^T \quad [\varepsilon] = [\varepsilon_x, \varepsilon_y, \varepsilon_z, \gamma_{yz}, \gamma_{xz}, \gamma_{xy}]^T$$

$$[D] = \frac{E}{(1+\mu)(1-2\mu)} \times \begin{bmatrix} 1-\mu & \mu & \mu & 0 & 0 & 0 \\ \mu & 1-\mu & \mu & 0 & 0 & 0 \\ \mu & \mu & 1-\mu & 0 & 0 & 0 \\ 0 & 0 & 0 & 0.5-\mu & 0 & 0 \\ 0 & 0 & 0 & 0 & 0.5-\mu & 0 \\ 0 & 0 & 0 & 0 & 0 & 0.5-\mu \end{bmatrix}$$

In the analysis of general finite element method, it can be solved by the method of minimum potential energy by using the viewpoint of potential potential energy, which must be satisfied for an elastic body:

$$E_p = U + W \tag{7}$$

In the finite element analysis, the main focus is that the scroll and the scroll tooth are combined by the pressure field and temperature field, so the relationship of stress changes should meet the following types:

$$\sigma = E(\varepsilon - \varepsilon_0) \quad \varepsilon_0 = \alpha\Delta T \tag{8}$$

The total internal strain energy of an object under analysis can be obtained by integral calculus:

$$U = \int_L \frac{1}{2}(\varepsilon - \varepsilon_0)^T E(\varepsilon - \varepsilon_0) A dx \quad \varepsilon = Bq; \quad dx = \frac{x_2 - x_1}{2} d\xi \tag{9}$$

B——Element strain displacement matrix.

$$U = \sum_e \frac{1}{2} q^T \left(E_e A_e \frac{l_e}{2} \int_{-1}^1 B^T B d\xi \right) q - \sum_e q^T E_e A_e \frac{l_e}{2} \varepsilon_0 \int_{-1}^1 B^T d\xi + \sum_e \frac{1}{2} E_e A_e \frac{l_e}{2} \varepsilon_0^2 \tag{10}$$

$$E_p = \frac{1}{2} Q^T K Q - Q^T F \quad \frac{\partial E_p}{\partial Q} = 0 \quad (11)$$

The displacement and stress value of each node of the scroll tooth can be calculated. Finally, the balance equation of the scroll tooth of the compressor is obtained by combining the above equations with [15].

4. Calculation Model

4.1. Establish 3D model

A 3D solid model of scroll scroll of oil-free scroll compressor was created by using Solidworks, and the medium in working chamber is air. The structural parameters of the scroll used as shown in table 1.

Table 1. Parameters of scroll

parameters	size
radius of base circle r_b	3.26mm
radius of gyration r	5.75mm
thickness of tooth t	4.5mm
height of tooth h	36mm
cylinder number N	4

In the analysis, the steady-state thermal analysis of the scroll is firstly carried out by Ansys, and the temperature variation of the scroll tooth is analyzed. Then the analysis results of the scroll were loaded into the static structure as thermal load field, and the coupled field was analyzed. Figure 1 shows a three-dimensional model of an air conditioning compressor rotor based on the above parameters.

4.2. Mesh generation

The mesh of Scroll plate of oil-free scroll compressor was generated by Ansys software. The material characteristics of the scroll disk are shown in the following table.

Table 2. Characters of ductile cast iron

material characteristics	Fe
modulus of elasticity E	173GPa
poisson ratio μ	0.3
density ρ	$7.8 \times 10^{-6} \text{ kg} / \text{mm}^3$
expansion coefficient α	$1.33 \times 10^{-5} / ^\circ\text{C}$
thermal conductivity λ	$0.0526 \text{ W} / \text{mm} \cdot ^\circ\text{C}$
specific heat C	$500 \text{ J} / \text{kg} \cdot ^\circ\text{C}$
tensile strength δ_b	400MPa
yield strength δ_{-1}	270MPa

Because the structure of the scroll disk is irregular, a free mesh method is adopted in order to get better mesh quality[16], Set its minimum cell size to 1 mm. Fig. 2 shows the mesh of the orbiting scroll.

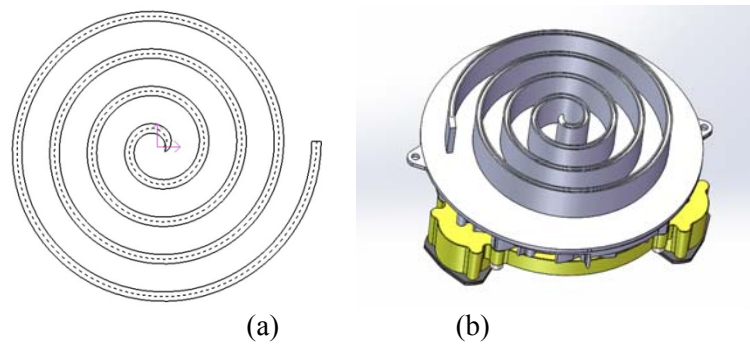


Fig. 1 The model of orbiting scroll

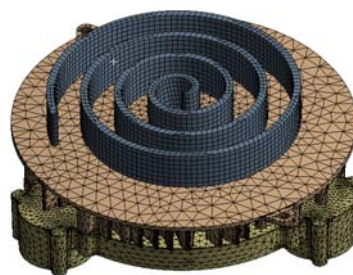


Fig. 2 The meshing model of orbiting scroll

4.3. Operation condition

The operation of the scroll compressor is determined by the input parameters of the motor, the structural parameters of the compressor and the environment at that time. Table 3 shows the operating conditions of the scroll compressor.

Table 3. The operation of compressor

Name	parameter
Intake pressure	0.1MPa(Absolute pressure)
Exhaust pressure	0.75MPa(Absolute pressure)
Intake temperature	20 °C
Isentropic index	1.41
Compression ratio	7.5
speed	3000 r/min

5. Analysis the result of Calculation

5.1. Deformation of a orbiting scroll in a temperature loading field

The constraint of the orbiting scroll is mainly limited by movement and rotation. The intake temperature of scroll compressor is set at room temperature 20 °C. The exhaust temperature is calculated by thermodynamic knowledge. According to the suction temperature and the exhaust temperature of the compressor, the temperature distribution of the orbiting scroll is analyzed. The overall distribution is affected by the exhaust temperature and the gas temperature, as shown in Figure 3 (a). Then the analysis results of the temperature distribution on the scroll tooth are loaded into the static analysis, thus the deformation distribution of the scroll tooth under the temperature load field

can be obtained, as shown in Figure 3 (b). It can be seen from Figure 3 that the deformation of the gear head at the initial end of the scroll of the compressor scroll is the largest, and the value is 0.1676mm. From the tooth head to the end of the tooth, the deformation of the tooth decreases as the temperature gradually decreases.

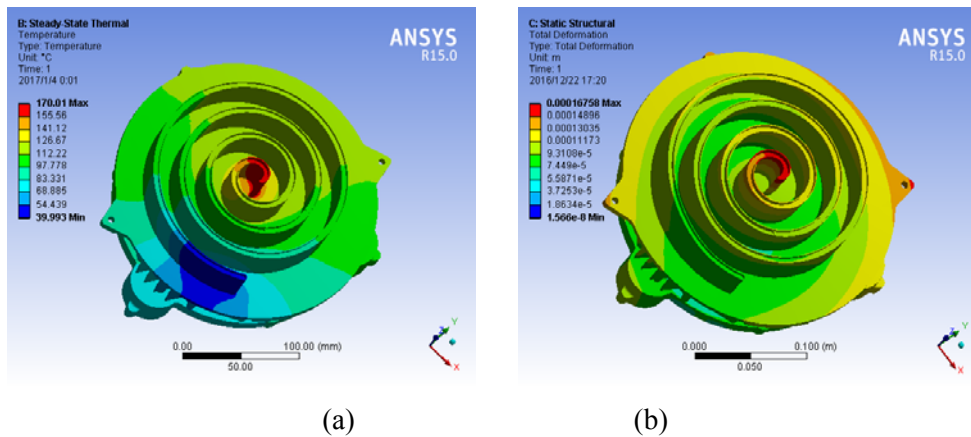


Fig. 3 Temperature distribution and thermal deformation of orbiting scroll

5.2. Deformation of orbiting scroll under gas force field

When the compressor is working, the pressure of the gas in the working chamber increases with the rotation of the main shaft until the exhaust stage reaches the maximum pressure. Because the pressure difference between the inner and the outer sides of the scroll tooth is different, the pressure difference is caused by the radial force acting on the scroll tooth. The pressure of the suction chamber is 0.1MPa, the average pressure of the first compression chamber is 0.14MPa, and the average pressure of the compression chamber is 0.26 MPa, and the center cavity pressure is 0.75MPa. The deformation under the gas load is shown in figure 4. It can be seen from the diagram that the deformation of the top of the gear head at the beginning of the scroll of the scroll gear is the largest, and the value is 0.0184mm.

5.3. Deformation of orbiting scroll under an inertial load field

The orbiting scroll plate through the eccentric spindle is connected with a belt wheel and the motor base circle center dynamic scroll around the fixed scroll for rotation and translation to scroll, so scroll plate will be deformed by the inertia force, which will cause the deformation of the scroll tooth. The deformation caused by the inertial load is shown in figure 5. From the figure, when the vortex disc is only inertia force field, the top end of scroll tooth deformation, the maximum deformation is 0.0002mm, which shows that the smaller the inertial load deformation effect on the scroll compressor, which can be neglected in general.

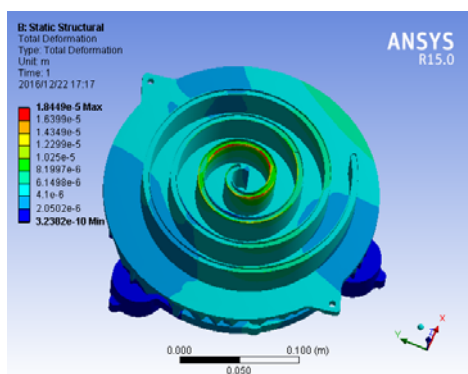


Fig. 4 The deformation under force loading

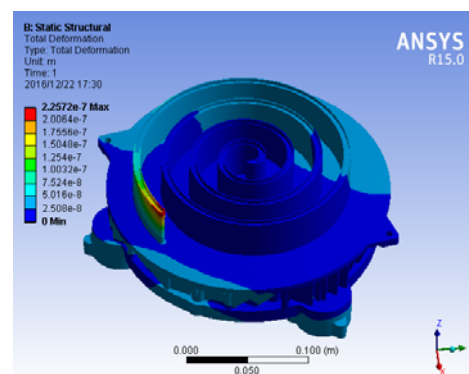


Fig. 5 The deformation under inertial loading

5.4. Deformation of scroll plate under coupling action

5.4.1. Deformation of orbiting scroll plate The force acting on the orbiting scroll plate is complicated under the actual working condition, the deformation of the compressor under actual working conditions can not be well analyzed only by analyzing the influence of a certain load on its deformation. When coupled with the physical field, the deformation distribution of the scroll is shown as shown in the following figure. It can be seen from Figure 6 that when the orbiting scroll plate is coupled, the deformation of the top of the initia of the scroll tooth is the largest, and the value is 0.168mm.

The arc length of the scroll tip of the orbiting scroll is changed into abscissa, and the deformation of the scroll tooth is taken as ordinate and the beginning of the scroll tooth is the coordinate origin established the coordinate system. The total deformation of the scroll tooth is obtained when the scroll plate of the compressor is loaded and coupled at each load field, as shown in figure 7. It can be seen from Figure 7 that the deformation of the coupled scroll is consistent with the variation of the deformation amount when the thermal load field is loaded separately. The maximum deformation occurs at the top of the scroll tooth, and the deformation of the scroll tooth decreases with the increase of the addendum arc length.

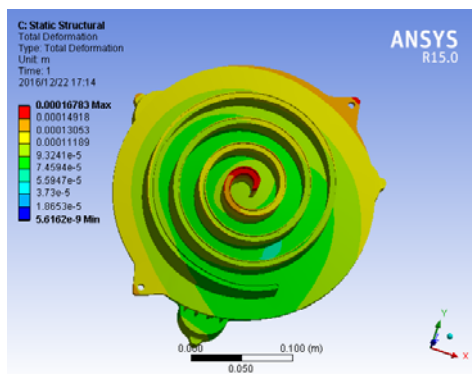


Fig. 6 The deformation under Coupling

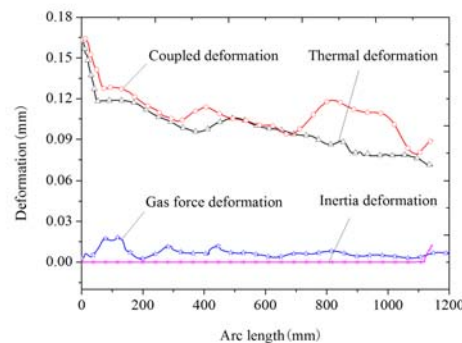


Fig. 7 The deformation under coupling effect

5.4.2. Meshing deformation analysis of scrolls The fixed scroll plate of the scroll compressor is connected with the frame by screw thread, so the screw hole and the positioning pin are arranged as the forced displacement constraint of the static vortex disc, and the displacement in the direction of X and Y is limited. The deformation of the fixed scroll plate under multi physical field coupling is analyzed, and its mesh and deformation are shown in Figure 8, as can be seen from the diagram, the deformation tendency of the fixed scroll plate is consistent with the orbiting scroll plate under the coupling action, because the stator disc is fixed with the frame and the thread and pin, almost no deformation occurs around it. The maximum deformation occurs at the beginning of the tooth end, and the value is 0.0173mm.

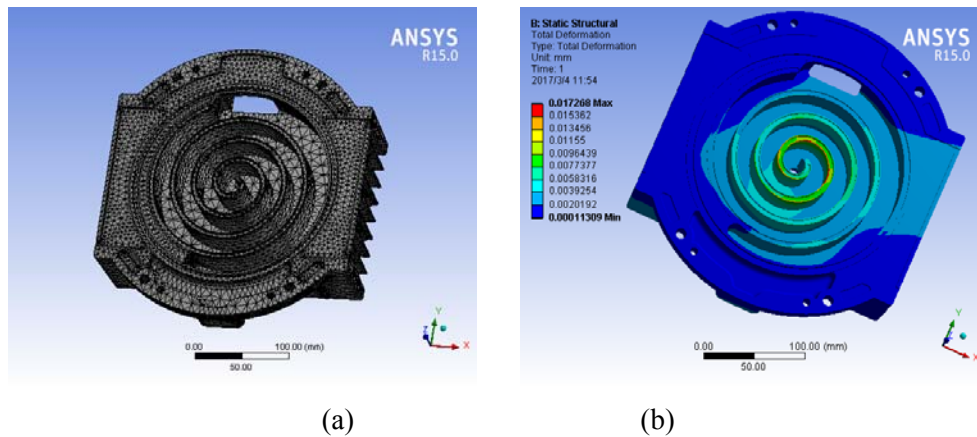


Fig. 8 The deformation of fixed Scroll

Figure 9 shows the comparison of the deformation of the scroll disk. The graph (a) is the curve of the deformation of the top of the orbiting scroll plate and the deformation of the root of the fixed scroll plate, and graph (b) is the change curve of the root of the orbiting plate and the deformation of the top of the fixed scroll. As can be seen from the diagram, the deformation of the fixed scroll plate is large than the orbiting scroll plate which the arc length is between 540mm and 590mm, In the graph (a), the difference is 0.0051mm, and the difference in the graph (b) is 0.0064mm. Here is the position of the first meshing point of the exhaust chamber just before end of the suction of the scroll. In order to avoid the collision of the two scroll gears during operation, the meshing gap between the scroll teeth is at least greater than the minimum difference.

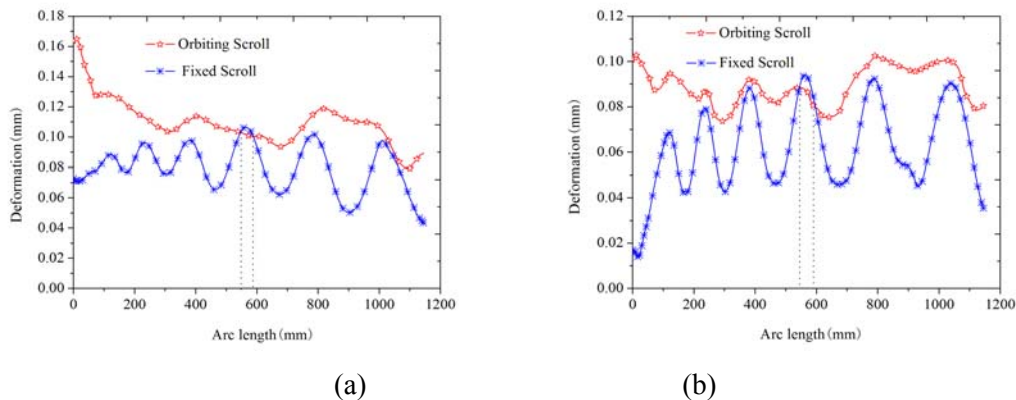


Fig. 9 The deformation contrast of Scrolls

5.5. Coupled deformation of orbiting scroll plate with different geometric parameters

In order to better understand the deformation of the orbiting scroll with different tooth thickness and different tooth heights under coupled physical field, different models are built and finite element analysis of the scroll is carried out. Because the orbiting scroll is moving part in the scroll compressor, and the force is complex, we choose only the orbiting scroll to establish different geometric parameters of the model. In Figure 10, the relationship between the deformation of the top of the scroll tooth and the length of the scroll tooth profile is given, and the maximum deformation occurs at the tooth head. It can be seen from the diagram that the deformation of the scroll tooth head has a certain relationship with the thickness of the tooth, which is that the thicker the scroll tooth, the smaller the deformation at the end of the tooth. Figure 11 shows the variation of the deformation of the top and inner wall and the length of the scroll line of the scroll teeth with different tooth heights. As can be

seen from the diagram, the deformation of the scroll tooth of the compressor has a certain relationship with the tooth height, which is that the higher the scroll tooth, the greater the deformation.

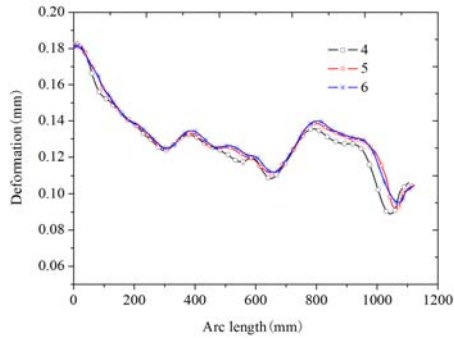


Fig. 10 The variable tooth thickness deformation

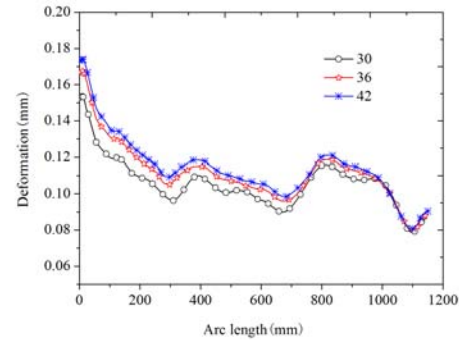


Fig. 11 The variable tooth height deformation

In order to ensure the strength and compression ratio of scroll compressor scroll, according to figure 10 and 11 shows that the tooth thickness of scroll teeth should be between 5~6mm, and the tooth height can be set to about 30mm.

5.6. Stress analysis of orbiting scroll plate under coupled field

As shown in FIG. 12, the stress distribution of the scroll plate in the coupling field is the coupling field. In the coupling field, the stress of the scroll plate is the largest at the edge of the inside of the bearing seat and the boundary of the end plate, next is the bottom of the gear head. The maximum stress is about 466.7MPa.

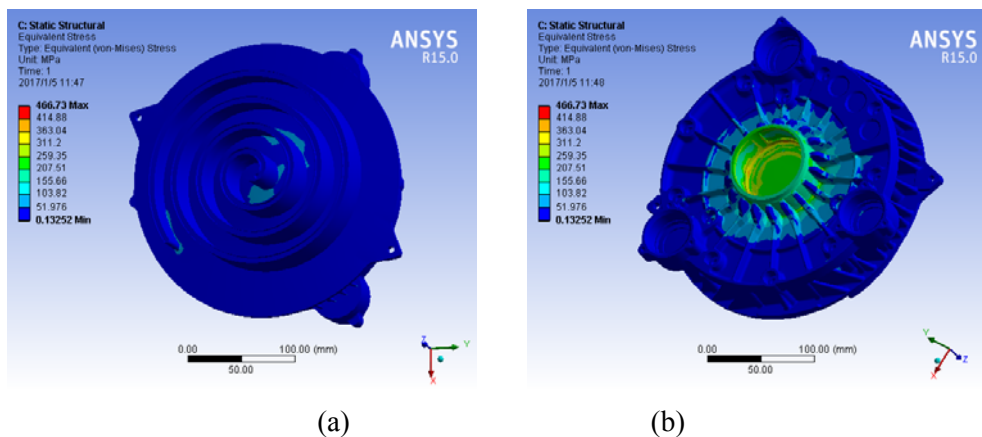


Fig. 12 The Stress distribution under Coupling

5.7. Experimental analysis

The oil-free scroll compressor was adopted in the experiment. The radial clearance of the assembly was set to 20 μ m, the axial clearance was set at 5 μ m, the tooth height was 36mm, and the tooth thickness was 5.8mm. The exhaust temperature and exhaust volume of scroll compressor can be measured by experiment, which can provide loading data for Ansys analysis. Figure 13 (a) is the test prototype, graph (b) is the schematic diagram of the experiment. and graph (c) as a test platform.

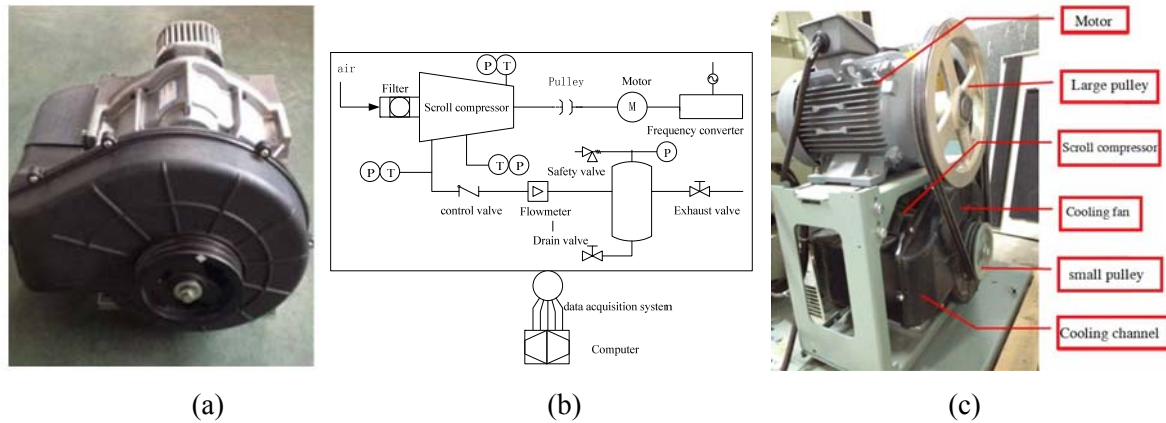


Fig. 13 The experimental test platform

Fig. 14 is a schematic diagram of the variation of the temperature with the rotation speed of the spindle when the oil-free scroll compressor is vented. The intake temperature of the scroll compressor is set to 20 °C at that time, and the exhaust gas pressure is 0.75 Mpa at the time of exhaust. As can be seen from Fig. 14, the exhaust temperature of the compressor increases with the increase of spindle rotation speed. With the increase of the spindle speed, the pressure difference of the gas in the adjacent cavity is reduced, so the amplitude is not large. The change of the temperature is in accord with the simulation analysis.

The theoretical exhaust volume of scroll compressor is the product of the stroke volume and the compressor speed:

$$Q_h = n\pi P(P - 2t) \left(2N - 1 - \frac{\theta_s}{180} \right) h \cdot \eta_v \quad \eta_v = \frac{Q_g \times 10^6 / n}{V_s}, \quad \theta_s = [N - \text{int}(N)] \times 360 \quad (12)$$

Figure 15 shows the variation of exhaust volume with rotational speed. It can be seen from the figure, the gas stays longer in the chamber at the low speed, and there is a large deviation between the calculated exhaust volume and the experimental data; while in high speed, the inhaled gas quickly discharged to the outside, therefore the simulated and experimental data are highly approximate.

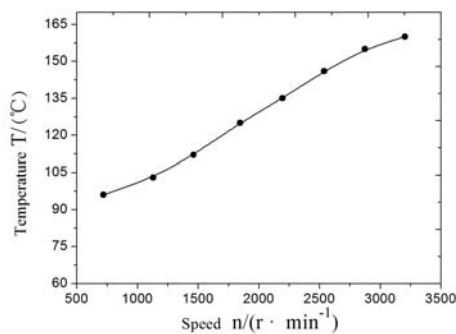


Fig. 14 Exhaust temperature with rotational speed

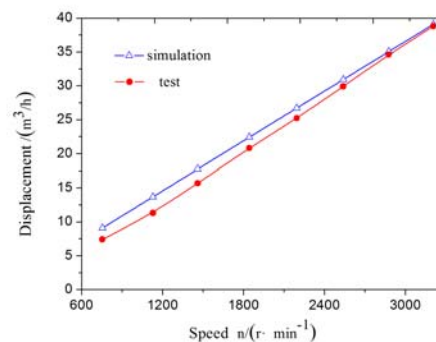


Fig. 15 The variation of exhaust volume with rotational speed

6. Conclusion

(1) The temperature load is the main load that influences the deformation of the scroll of the orbiting scroll. The maximum deformation is at the head of the scroll tooth, and the deformation decreases gradually with the increase of the addendum arc length.

(2) The effects of gas force and inertia load on the deformation of scroll tooth in oil-free compressor are less. Because the pressure of the gas in each chamber is different, there will be different amplitudes of deformation, and the greater the pressure difference between the two sides of the cavity, the greater the variation of deformation.

(3) Under the coupling field, the deformation of the scroll of the scroll plate with different teeth height and tooth thickness is different, the higher the tooth and the smaller the tooth thickness, the greater the deformation.

(4) The stress of the compressor scroll is concentrated at the contact between the tooth head and the bottom plate, and the maximum stress of the coupling field is not the linear superposition of the stresses when the loads are individually loaded. The modification of the scroll tooth head can reduce the stress concentration at the end of the tooth.

7. Nomenclature

T_s —Inspiratory temperature	P_d —Exhaust pressure	P_s —Inspiratory pressure	P —
Involute pitch			
ϕ_e —Terminal opening angle	a —acceleration	ϕ —Involute spread angle	n —
speed			
θ —Spindle angle	θ^* —Start exhaust angle	φ —Central angle of arc	V_s —
Inspiratory volume			
E_p —Total total potential energy	A_e —Cell area	U —Internal strain energy	l_e —
Element length			
W —Work done externally	Q_g —Exhaust volume	ε_0 —Thermal strain resulting from	
changes in temperature;			
ΔT —Temperature change	E_e —Element potential energy	q —Displacement vector of	
element node			
η_v —Volume efficiency	θ_s —End of inspiratory angle	$\text{int}(N)$ —Integral function	

Acknowledgements

This work supported by National Natural Science Foundation of China (Grant No. 51275226, 51675254), Project supported by the young Longyuan innovation team

References

- [1] LIU Z Q. The Scroll Fluid Machinery and Scroll Compressor [M]. China Machine Press,2009.
- [2] PENG B, SUN Y. Mathematical model and experimental study of variable-section scroll compressor [J]. Chinese Journal of Mechanical Engineering, 2015, (14): 185-191.
- [3] Peng Bin, Arnaud Legros, Vincent Lemort ,XieXiaozheng, Gong Haifeng. Recent Advances on the oil-free Scroll Compressor [J].Recent Patents on Mechanical Engineering. 2016, 9(1): 37-47.
- [4] LIU G P, ZHANG G L. Deformation and Stress Simulated Analysis of Orbiting Scroll Under the Coupling Function [J]. Chinese Hydraulics & Pneumatics, 2016, 5(12): 60-64.
- [5] JIN D, CHEN X, TIAN T. Stress and Deformation Analysis of Orbiting Scroll in Scroll Compressor under Inhomogeneous Temperature Field [J]. Fluid Machinery, 2003, 31(6): 11-14.
- [6] HUANG L, TANG J C, HAN K. The effect of temperature field on the stress and strain of

- orbiting scroll [J]. *Cryogenics and Superconductivity*, 2013, 41(5): 60-63.
- [7] LI C, XIE W J, ZHAO M. Deformation and Stress Analysis of Orbiting Scroll Under the Multi-field Coupling [J]. *Fluid Machinery*, 2013, 41(8): 16-20.
- [8] LI C, YU Y, ZHAO M. Virtual Modeling and Dynamic Simulation of Scroll Compressor [J]. *Fluid Machinery*, 2012, 40(1): 26-30.
- [9] LI C, XIE W J, ZHAO M. Finite Element Analysis of the Influence of Different Loads and Structures on the Stress of the Scroll Wrap [J]. *Chinese Journal of Mechanical Engineering*, 2015, 51(6): 189-197.
- [10] YIN J, YANG M C, FENG J. The Finite Element Analysis of Dynamic Vortex Plate of Scroll Compressor Based on Thermal Stress Field Coupling[J]. *Compressor Technology*, 2011, (6): 6-9.
- [11] GUO R N, WANG R X, FENG X W. Scroll Plate Numerical Simulation for Scroll Compressor[J]. *Chemical Engineering & Machinery*, 2011, 38(3): 345-347.
- [12] WANG J, ZHANG N, LIU K. Stress and Deformation Analysis on Wraps in Scroll Compressor Based on Flow Field Simulation[J]. *Journal of Engineering Thermophysics*, 2012, 33(8): 1334-1337.
- [13] YANG G Y, SHENG L, ZHANG Xiuli. ANSYS simulation of temperature field, stress field and thermal deformation of vacuum oil-free scroll pump [J]. *vacuum*, 2008, 45(5): 17-19.
- [14] PENG B. The research on twin-spirals scroll compressor based on modern design methods [D]. Lanzhou: Lanzhou University of Technology, 2007.
- [15] HE W B, ZENG P, ZHANG L. Pre-stress Test for Steel Wire Wound Moving Beam of Heavy Forging Press Based on Finite Element Method[J]. *Chinese Journal of Mechanical Engineering*, 2012, 48(10): 66-67.
- [16] CAO H J, SHU L S, XU Lei. Hexahedral Mesh Generation Method for Complex Mechanical Structure [J]. *Chinese Journal of Mechanical Engineering*, 2014, 50(15): 113-118.